PENETRATION OF LATERALLY QUANTIZED FLUX LAMINA INTO A SUPERCONDUCTING WIRE NETWORK

H. D. Hallen*
Dept. of Physics, North Carolina State University, Raleigh, N.C. 27695-8202
and
A. M. Chang, R. Miller, L.N. Pfeiffer,
K. West, and H. F. Hess

AT&T Bell Laboratories, Murray Hill, N.J. 07974-0636

We report direct, high resolution images of the magnetic field above a superconducting wire grid as applied flux penetrates into an initially empty state or into a state with half the plaquettes containing a magnetic quantum. We find two qualitatively different initial approaches to equilibrium: in wide structures for the former, or with long, linear structures for the latter case. In the approach to a empty state, we observe the formation of residual quasi-bound magnetic vortex/anti-vortex pairs.

KEYWORDS: A Superconductors, C Scanning probe microscopy
D Flux pinning and creep

The motion of magnetic flux lines or vortices within superconductors has received considerable interest, from both an experimental and theoretical viewpoint. Only recently has the penetration of magnetic vortices into a uniform type II superconducting sample been addressed from a theoretical [1] viewpoint. Most experimental efforts have probed the time-dependent magnetization of samples, which yields averaged bulk values. Such measurements suffer from insensitivity to both the large scale spatial flux distribution and the arrangement of individual vortices. Recently, electron holography [2] studies have produced real-space images of local vortex arrangements and motion in type I superconducting films, where pinning at random sites was found to be important. Studies using a magneto-optical detection [3] have yielded real-time images of flux dendrite growth in type II superconducting films. Scanning Hall probe studies [4] have yielded high resolution images on similar films. Other systems, two-dimensional superconducting wire networks, are fascinating from an experimental point of view, however, as they can be extremely well-controlled. The ability to vary experimental parameters, such as the size and symmetry of the network and the flux per unit cell f, makes these networks attractive and convenient for detailed investigation. Scanning Hall probe microscopy [5] is one of several recent techniques [6] with the sensitivity and resolution to image the real-space vortex configuration in such systems. This opens new venues for these systems which have been studied extensively with other techniques in the past decade.[7-11] In particular, we are now able to investigate the flux penetration and nucleation of the ordered vortex states in these networks from an initial state which is very different from the final state, i.e., we can produce far from equilibrium states and observe their relaxation. The real space images show whether or not flux penetrates uniformly along the edge of these samples as might be expected, for example, in the well-known Bean model [12], and may give insights related to the vortex avalanches reported in reference 7.

In this paper we present direct scanning Hall probe observations of the vortex configurations in a superconducting wire network as the vortex system is relaxed in steps from an initially ordered state with fraction of lattice sites filled f_i to a final ordered state with f_f. We concentrate on the cases $(f_i, f_f) = (1/2, 0)$ and $(0, 1/2)$. For the $f = 1/2$ state, the magnetic field is

such that half of the grid holes contain a vortex [13], in a checkerboard pattern, whereas the lattice is empty in the f = 0 state. It is found that the initial steps are characterized by the growth of structures of high magnetic field due to the influx of either multiple vortices or multiple anti-vortices [14] into a row of single lattice holes. The spatial distribution of the influx is not symmetric as f_i and f_f are alternated between 0 and 1/2.

The sample used was a 100 μm × 200 μm grid of 0.95 μm × 0.95 μm square holes formed of 0.25 μm wide Nb wires fabricated by patterning a 1000 Å thick Nb film using electron beam lithography and reactive ion etching. The Nb has a superconducting transition temperature T_C = 8.8 K at B = 0 G, a room temperature resistivity of 1.5 ohms/square and a resistivity ratio at 300 K to 10 K of ~2. To test sample quality and calibrate the applied perpendicular magnetic field B we performed in-situ four-point transport measurements. The measured variation of T_C as a function of B is similar to previous reports:[15] T_C is periodic in the field B = 22.6 G corresponding to f = 1 with sub-structures at f = 1/2 and f = 1/3. The initially ordered vortex states, as discussed in Ref. 5, were prepared by cooling the sample slowly (~ 1 mK/sec) in the applied field B to below T_C. Scanning Hall probe microscope [4] is used to detect the local magnetic field above the sample. The probe, a GaAs heterostructure patterned into a (0.3 μm junction size) Hall bar by electron beam lithography, was positioned 0.22 μm above the sample surface and then raster scanned to record the local-field induced Hall voltage. The range of the scanner allows ~400 lattice points to be imaged. The right side of the images shown here were fairly close (tens of μm) to an edge of the physical grid. The physical lattice is rotated ~11° clockwise from the image orientation. The far from equilibrium states were formed by first

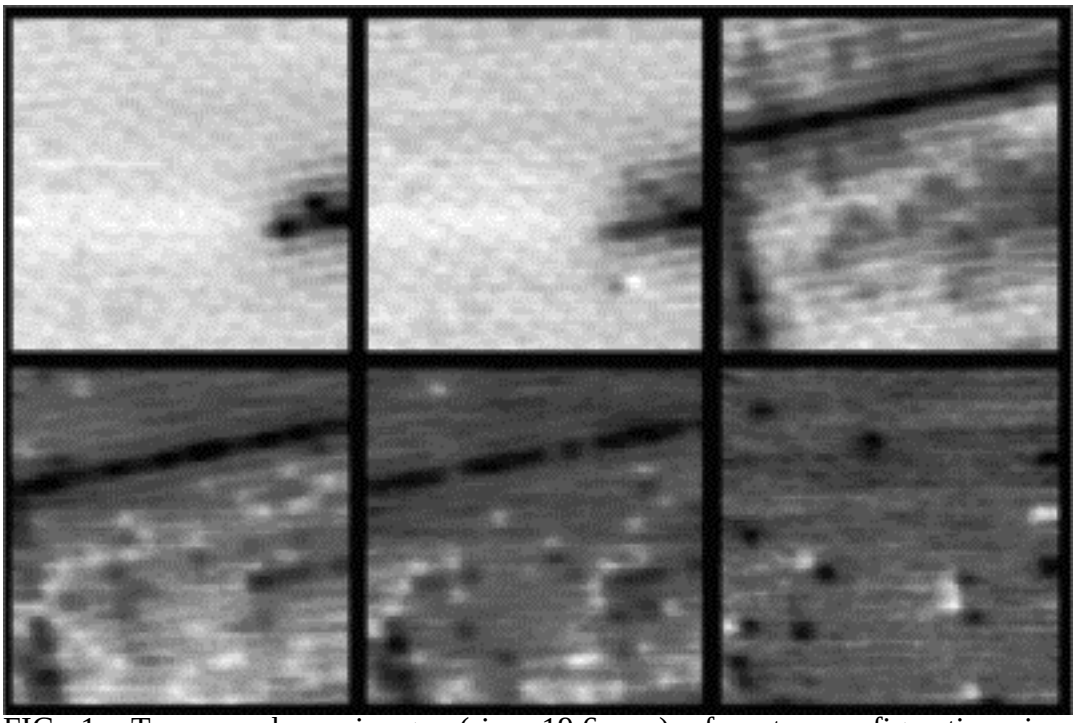

FIG. 1: Top row shows images (size: 19.6 μm) of vortex configurations in a superconducting Nb wire grid . The sample was prepared in a half-filled checkerboard state, then the external magnetic field removed with the temperature at 5°K, i.e., a f = 1/2→0 transition. The images with indicated gray scale magnetic field range were taken at 5K after heating to (a) no heating, -25 to 15 gauss (b) 7.5K, -20 to 15 gauss (c) 8.25K, -12 to 15 gauss (d) 8.50K, -10 to 10 gauss (e) 8.62K, -8 to 8 gauss and (f) 8.69K, -5 to 5 gauss. T_c (midpoint) for the Nb in the grid lines is ~8.8K. Vortices are light, anti-vortices are dark.

preparing an ordered $f_i = 1/2$ (or 0) state, cooling to 5°K, then adjusting the final field for a final state $f_f = 0$ (or 1/2). Assuming no relaxation, this produces fields $B_{ext} < B_{int}$ (or $B_{int} < B_{ext}$). To image the relaxation, the following steps are repeated: image, raise the temperature for a fixed time period (~10 min), re-cool to 5°K, image. The images were acquired well below T_c where the vortex configurations are stable over imaging times and the shorter penetration depth of Nb enhances the magnetic contrast.

The metastable states at each temperature represent the ability of the system to approach the ground state given the thermal energy and superconductor properties at that temperature. One can heuristically consider the reduction of superconducting critical current with increasing temperature to yield a lower, temperature dependent barrier height for vortex motion. The vortices are driven over the barrier by local magnetic field gradients. Snapshots of the process by which the system converts from $f_i = 1/2$ to $f_f = 0$ is illustrated in Fig. 1. It is initially (Fig. 1(a-c)) characterized by the influx into the ordered checkerboard lattice [9] from a nearby edge of high flux structures along single lattice constant wide lines ("cracks"). The maximum field in these cracks is ~50 gauss compared to ~10 gauss in the f = 1/2 regions. This corresponds to about 4-5 anti-vortices per plaquette. Note that several of these "cracks" are observed across the image, and the checkerboard vortex state remains between. With higher temperature annealing, the "crack" propagates, Fig. 1(d-f), and the anti-vortices spread laterally where they annihilate vortices. The initial stages or the relaxation of $f_i = 0$ to $f_f = 1/2$ are qualitatively different. This is shown in Fig. 2. The multiple-vortex-in-a-lattice-site structure penetrates along the lattice diagonals. A broader region around this also shows enhanced flux. As before, the flux spreads laterally at temperatures approaching T_c, and converts to an ordered checkerboard pattern upon annealing very near T_c.

The general properties of the initial influx of anti-vortices in Fig. 1 or vortices in Fig. 2 are driven by the macroscopic demagnetization field distribution above the sample surface. Once nucleated at some influx region, the (anti-)vortices propagate in straight lines, branching and

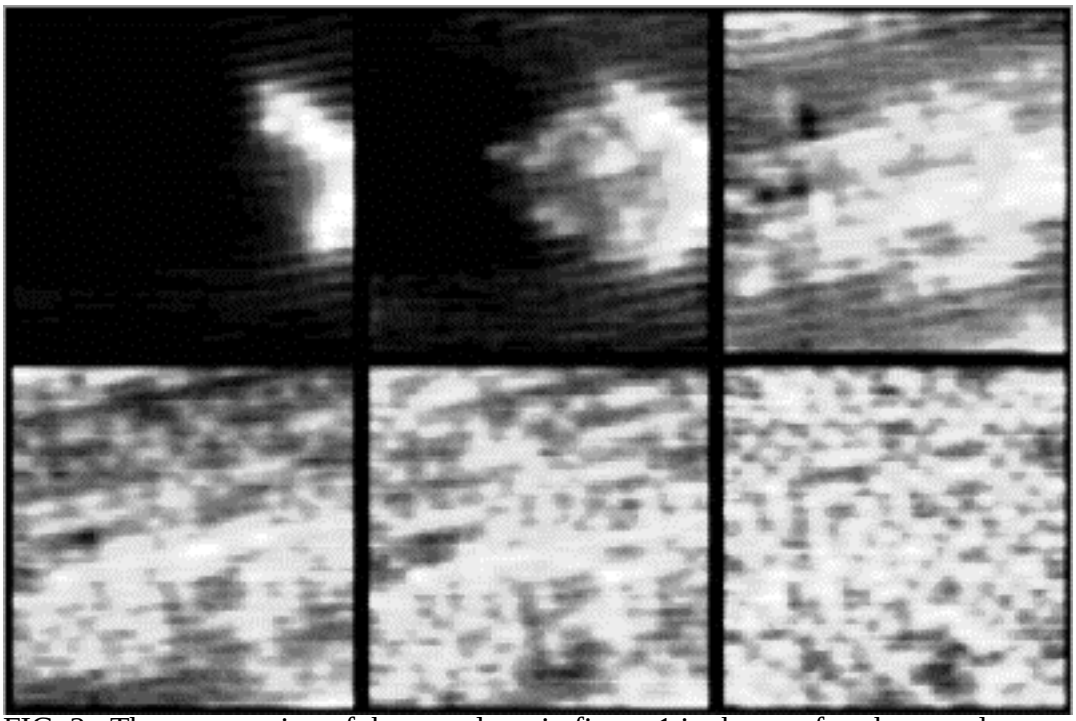

FIG. 2: The same region of the sample as in figure 1 is shown after the sample was prepared with a $f = 0 \rightarrow 1/2$ transition at 5K. The images with indicated gray scale field range were taken at 5K after heating to (a) no heating, 0 to 45 gauss (b) 7.5K, 0 to 27 gauss (c) 8.25K, 1 to 20 gauss (d) 8.50K, 2 to 18 gauss (e) 8.62K, 3 to 16 gauss and (f) 8.69K, 6 to 15 gauss ,i.e., the same temperatures as figure 1.

spreading laterally only at higher temperatures where barriers to motion are much smaller. A reason for this has been suggested by Huebner [16] in reference to flux penetration in type 1 superconductors, but the same general argument also applies here. Briefly, current is enhanced and approaches the critical current at the tip of the (anti-)vortex finger penetrating the grid. This reduces the barrier for (anti-)vortex motion in the forward direction and hence favors the creation of long, linear vortex penetration lines, as are observed in both figures 1 and 2. Based on limited data, we suspect the direction of penetration, along the grid for an f = 1/2 background or diagonal into an empty state, may be generic.

An interesting, qualitative comparison between the figures, from an inhomogeneous grid, and a model calculation [1], of a uniform initial superconductor, can be made. The model [1] shows a vortex penetration structure consisting of several discontinuous parallel and perpendicular lines into the sample. This is in qualitative agreement with the observations of the initial flux penetration here. We should also compare these qualitative properties with related (but different) vortex filled dendrites recently observed experimentally in uniform type II superconducting films [3]. In contrast to the curved and widely branching structures described in the reference, the structures shown here in a type II grid structure are unique in several respects: (1) The width is exceedingly narrow -- confined primarily in a single plaquette wide strip, the smallest quantum. (2) The fields within this strip are very intense -- an order of magnitude higher than the externally applied field. (3) A family of parallel lines neighbor the flux profusion, suggesting significant currents on grid wires several lattice constants away. (4) It appears that different initial flux penetration directions, along a row or a diagonal, are produced depending upon the initial field profile.

The driving forces become much more local and the increasing temperature reduces the barriers to vortex motion in the later stages. The f: $0 \rightarrow 1/2$ case has been discussed previously [5]. An image from the latter stages of f: $1/2 \rightarrow 0$ is shown in figure 2f. Note the large density of vortex/anti-vortex pairs separated by one unit along the diagonal (recall the grid is rotated from the image). These pairs persist until the sample is annealed to within a few percent of the superconducting transition temperature T_c, after which an empty state is obtained. The vortex/anti-vortex pairs along a diagonal are the result of the interplay between their attractive interaction and the barrier to their motion supplied by the lattice. It appears that at temperatures within about 0.2°K of the transition temperature, the pair attraction is strong enough to overcome the barriers and move closer to each other. A diagonal neighbor is metastable since it must first move into an adjacent site (lower driving force) before it can hop a narrow wire and annihilate. Hence the diagonal vortex/anti-vortex pairs are metastable closer to T_c than other pair configurations.

One can use the temperature T at which the diagonal neighbors annihilate as a measure of the energy barrier to vortex motion. Our estimation neglects supercurrent energies and uses a coarse monopole approximation for the external fields. We find an energy barrier for motion through a wire of $\Delta E = 0.013$ eV. This can be compared with an independent estimate from calculations in Josephson junction arrays [17]: $\Delta E \sim 0.2\ \phi_0/(2\pi)\ I_c(0)\ [1 - (T/T_c)^4]^{3/2}$. Using $I_c(0) = 0.0025$ A/wire measured by studying the onset of vortex motion with applied current, we find $\Delta E = 0.0037$ eV at T. Better agreement would require a calculation including the details of the grid.

In summary, we report real-space measurements of vortex configurations in a square wire lattice when the system is exposed to a large applied field change while at low temperature. The approach to the equilibrium configuration is imaged in steps. Images show that the uniform flux penetration assumed by the Bean model is not valid. We observe flux protrusions that are laterally quantized and find a qualitative difference in the initial approach to equilibrium between $f = 1/2 \rightarrow 0$ and $f = 0 \rightarrow 1/2$. The latter stages of the approach to $f = 0$ invite the appearance of a local metastable construction: a vortex and an anti-vortex as diagonal nearest neighbors.

REFERENCES

1. Holger Frahm, Salman Ullah and Alan T. Dorsey, Phys. Rev. Lett. **66**, 3067 (1991).
2. K. Harada, et al, Phys. Rev. Lett. **71**, 3371 (1993).
3. C.A. Durán, P.L. Gammel, R.E. Miller, and D.J. Bishop, Phys. Rev. Lett**. 74**, 3712 (1995); Nature (London) **357**, 474 (1992).
4. A.M. Chang, et al., Appl. Phys. Lett. **61**, 1974 (1992); A. M. Chang, et al., Europhys. Lett. **20**, 645 (1992); and H.D. Hallen, et al., SPIE Proceedings **1855** (1993).
5. H.D. Hallen, et al., Phys. Rev. Lett. **71**, 3007 (1993).
6. L.N. Vu, M.S. Wistrom, and D,J, Van Harlingen, Appl. Phys. Lett. **63**, 1693 (1993).
7. Stuart Field, Jeff Whit, Franco Nori, and Xinsheng Ling, Phys. Rev. Lett. **74**, 1206 (1995).
8. Thomas C. Halsey, Phys. Rev. **B31**, 5728 (1985); S. Teitel, Physica **B152**, 30 (1988); J. Villain, J. Phys. **C10**, 1717 (1977).
9. S. Teitel and C. Jayaprakash, Phys. Rev. **B27**, 598 (1983) and Phys. Rev. Lett. **51**, 1999 (1983).
10. Mohammad R. Kolahchi and Joseph P. Straley, Phys. Rev. **B43**, 7651 (1991).
11. C.J. Lobb, Physica **B152**, 1 (1988) and the other papers in this special issue; M.A. Itzler, et al. Phys. Rev. **B42**, 8319 (1990) and the first 4 references therein.
12. C.P. Bean, Phys. Rev. Lett. **8**, 250 (1962).
13. The magnetic flux of a vortex is quantized in type II superconductors with magnitude equal to one flux quantum = ϕ_0 = 20.7 Gauss micron^2.
14. An anti-vortex is a vortex with the magnetic field pointing out the other side of the sample.
15. M.S. Rzchowski, S.P. Benz, M. Tinkham, and C.J. Lobb, Phys. Rev. **B42**, 2041 (1990).
16. P.P. Huebner, "Magnetic Flux Structures in Superconductors," (Springer Verlag, Berlin, 1979).
17. J.R. Phillips et al, Phys. Rev. B**47**, 5219 (1993); and C.J. Lobb, D.W. Abraham and M. Tinkam, Phys. Rev. B**27**, 150 (1983).